

# Study of Al-doped ZnO Transparent Stimulus Electrode for Fully Implantable Retinal Prosthesis with Three-dimensionally Stacked Retinal Prosthesis Chip

Hisashi Kino,<sup>1</sup> Takafumi Fukushima,<sup>2</sup> and Tetsu Tanaka<sup>2,3\*</sup>

<sup>1</sup>Frontier Research Institute for Interdisciplinary Sciences, Tohoku University,  
6-6-12 Aza-Aoba, Aramaki, Aoba-ku, Sendai, Miyagi 980-8579, Japan

<sup>2</sup>Graduate School of Engineering, Tohoku University,  
6-6-12 Aza-Aoba, Aramaki, Aoba-ku, Sendai, Miyagi 980-8579, Japan

<sup>3</sup>Graduate School of Biomedical Engineering, Tohoku University,  
6-6-12 Aza-Aoba, Aramaki, Aoba-ku, Sendai, Miyagi 980-8579, Japan

(Received September 14, 2017; accepted November 30, 2017)

**Keywords:** retinal prosthesis, 3D-IC, stimulus electrode, Al-doped ZnO

To realize a three-dimensionally (3D) stacked retinal prosthesis chip having a large stimulus electrode area and a large photodiode area, the fundamental properties of an Al-doped ZnO transparent stimulus electrode were investigated in detail. The test samples were fabricated, and thin film property and stimulus electrode characteristics were also evaluated using several methods. It was clearly observed that both the crystallinity and transmittances of an Al-doped ZnO thin film were dependent on the substrate temperature during thin-film formation. A better crystallinity and a transmittance of more than 85% in the visible range were achieved for the Al-doped ZnO thin film with a substrate temperature of 200 °C. Furthermore, good electrochemical impedance characteristics and adequate charge injection capacity (CIC) values of 0.07 mC/cm<sup>2</sup> were obtained to elicit visual sensations. Consequently, Al-doped ZnO has the possibility of becoming the transparent stimulus electrode for a 3D stacked retinal prosthesis chip.

## 1. Introduction

Recently, with the progress of the aging society, the number of blind patients has been remarkably increasing worldwide. In particular, many people lose their vision owing to ocular diseases such as cataract and glaucoma in developing countries, because medical treatments have not sufficiently progressed in such countries. On the other hand, effective medical treatments for retinal diseases such as retinitis pigmentosa (RP) and age-related macular degeneration (AMD) have not been established yet even in industrialized countries. More than 10 million people are blind owing to these retinal diseases worldwide.<sup>(1)</sup> Photoreceptor cells in the retina play a very important role and convert incident light signals into electrical signals. In the retina of blind patients with RP or AMD, photoreceptor cells are almost or sometimes

---

\*Corresponding author: e-mail: ttanaka@bme.tohoku.ac.jp  
<http://dx.doi.org/10.18494/SAM.2018.1741>

completely absent. However, in most cases, retinal cells such as bipolar cells and ganglion cells often remain normal even in blind patients with RP and AMD, and it was confirmed that light perception can be elicited by electrical stimulation to the remaining visual pathway.<sup>(2)</sup> In other words, it will be possible to restore one's visual sensation by stimulating the remaining retinal cells. In recent years, several visual prostheses have been developed worldwide.<sup>(3–5)</sup> We have also developed a fully implantable retinal prosthesis with a three-dimensionally (3D) stacked retinal prosthesis chip.<sup>(6,7)</sup>

Figure 1 shows a conceptual drawing of the fully implantable retinal prosthesis. The implantable retinal prosthesis is composed of extraocular and intraocular devices, which are connected by a telemetric inductive link. The extraocular devices consist of a primary coil and a transmitter for power transmission. The intraocular device consists of the 3D stacked retinal prosthesis chip, a flexible printed cable (FPC) with a stimulus electrode array, and a secondary coil for power reception. The 3D stacked retinal prosthesis chip is attached to the FPC. In the 3D stacked retinal prosthesis chip, a photoreceptor chip, an image processing circuit chip, and a stimulus current generator chip are vertically stacked and electrically connected by many through-Si vias (TSVs) formed in a Si substrate. By implanting the 3D stacked retinal prosthesis chip into the eyeball, the patients can employ their own lens and cornea, and can shift a gaze point by moving the eyeball, leading to high-speed visual information processing by using saccadic effects. As the 3D stacked retinal prosthesis chip has a layered structure similar to the human retina, more than 1000 pixels can be fabricated in the retinal chip. This leads to a small chip size, light weight, large fill factor, high resolution, and the resultant high quality of life (QOL) for the patients.

In general, there are three types of electrical stimulation to the retina, namely, epiretinal stimulation, subretinal stimulation, and suprachoroidal transretinal stimulation.<sup>(8–13)</sup> Figure 2 shows configurations of an epiretinal stimulation and a subretinal stimulation with the 3D stacked retinal prosthesis chip. The 3D stacked retinal prosthesis chip receives incident light and converts it into a biphasic stimulus current train, and the stimulus electrode array stimulates the remaining retinal cells. Each stimulation method has advantages and disadvantages. In the epiretinal stimulation, the FPC with the stimulus electrode array is placed below the stimulus

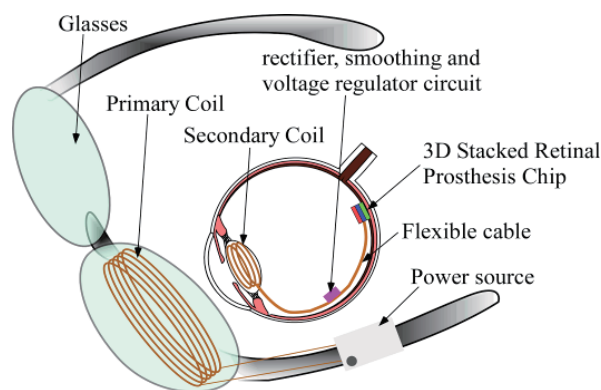


Fig. 1. (Color online) Configuration of fully implantable retinal prosthesis with 3D stacked retinal prosthesis chip.

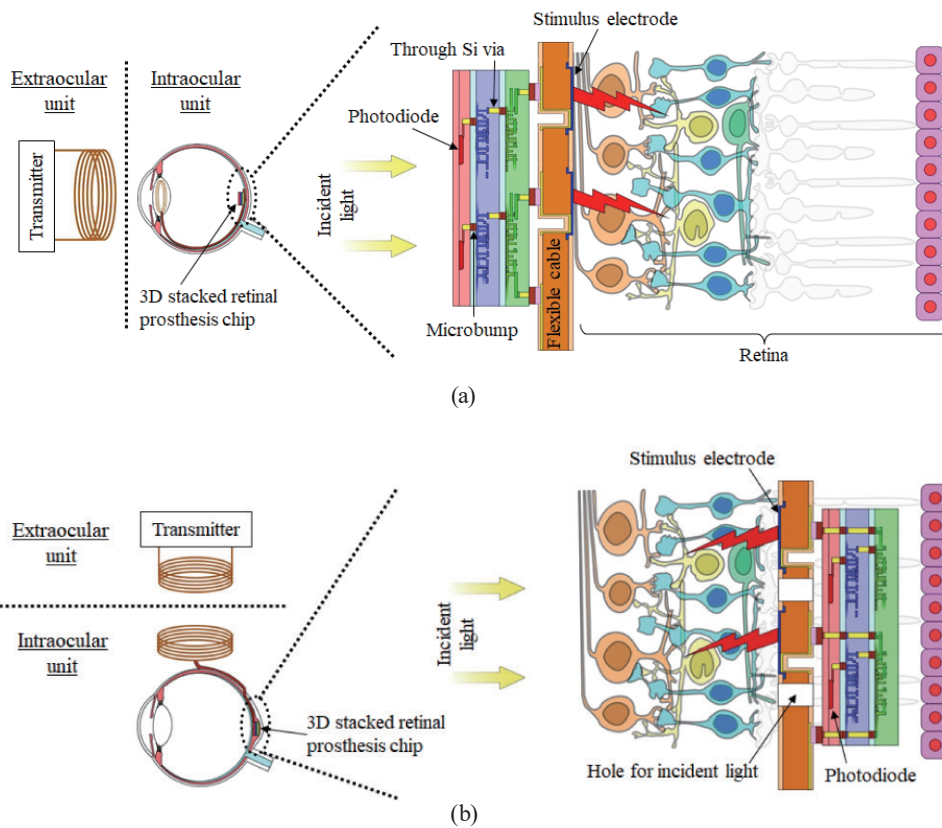


Fig. 2. (Color online) Configuration of (a) an epiretinal stimulation and (b) a subretinal stimulation with the 3D stacked retinal prosthesis chip.

current generator chip, that is, the opposite side of the photoreceptor chip. In the subretinal stimulation, as the FPC with the stimulus electrode array is placed on the photoreceptor chip, there are many holes in the FPC so that the incident light goes through the FPC and reaches the photodiodes. From the viewpoint of surgery, it is more difficult for the epiretinal stimulation to implant and fix the retinal prosthesis chip inside an eyeball, compared with the subretinal stimulation. However, for the subretinal stimulation, part of the incident light is blocked by the stimulus electrodes on the FPC, which leads to a small photodiode area and the resultant low-sensitivity retinal prosthesis chip. Meanwhile, a large photodiode area reduces the stimulus electrode area, which leads to a small stimulus current. One of the solutions to this problem is to fabricate the stimulus electrode array using transparent materials. In this paper, to realize the large stimulus electrode area and large photodiode area simultaneously, the fundamental characteristics of the transparent stimulus electrode are studied for high QOL retinal prostheses.

## 2. Method for Evaluation of Al-doped ZnO Transparent Stimulus Electrode

The transparent electrodes have been developed for a long time and are widely used for solar cells, flat panel displays, touch panels, and so on. Until now, several materials such as diamond,

indium tin oxide (ITO), and zinc oxide (ZnO) have been commercially used as the transparent electrodes. There are several requirements for the transparent material used for implantable stimulus electrodes, that is, biocompatibility, optical transmittance in visible wavelength range, and charge injection capacity (CIC). ITO is not appropriate for the stimulus electrodes as In is toxic to the human body.<sup>(14)</sup> Meanwhile, diamond is a material with good biocompatibility. However, a Si seed layer or high-temperature process is required for the deposition of diamond.<sup>(15)</sup> Stimulus electrodes are formed on an LSI chip. Therefore, we cannot use a diamond that needs a seed layer or a high-temperature process. ZnO is nontoxic and widely used in cosmetics, dental treatment, and other biological uses.<sup>(16)</sup> In addition, ZnO can be deposited by a low-temperature process without a seed layer. The conductivity of ZnO can be changed in accordance with the doping concentrations of Ga or Al into ZnO.<sup>(17)</sup> In this study, Al-doped ZnO (AZO) was used to evaluate fundamental characteristics from the viewpoint of availability as the transparent stimulus electrode.

The test samples were fabricated, and the thin film property and stimulus electrode property were evaluated. Figure 3 shows a fabrication process flow of the test sample for characterization. A 2-in. Si wafer of 280  $\mu\text{m}$  thickness was used for the test sample fabrication. First, a 1- $\mu\text{m}$ -thick  $\text{SiO}_2$  layer was deposited on the Si wafer by plasma-enhanced chemical vapor deposition (PECVD). Next, Ti/Au/Ti wires with thicknesses of 15/300/15 nm were formed by sputtering and photolithography. A 1- $\mu\text{m}$ -thick  $\text{SiO}_2$  layer was also deposited by PECVD. After the opening of contact holes and connection pads, Al-doped ZnO of 300 nm thickness was formed by sputtering and photolithography. An AZO sputtering target has a weight percent ratio of  $\text{Al}_2\text{O}_3$  to ZnO of 2%. Several substrate temperatures were used during Al-doped ZnO sputtering to investigate the appropriate sputtering conditions. The substrate temperatures were set to 100, 200, and 300  $^\circ\text{C}$ , and no heating. The sputtering process was performed using Ar under a 0.5 Pa pressure. Two sets of the test samples were fabricated in the Si wafer. Photographs of the fabricated test sample in the half Si wafer are shown in Fig. 4. The

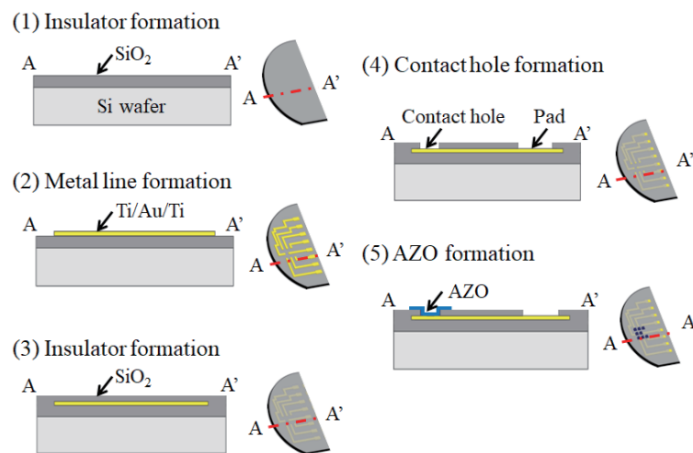


Fig. 3. (Color online) Fabrication process flow of the test sample.

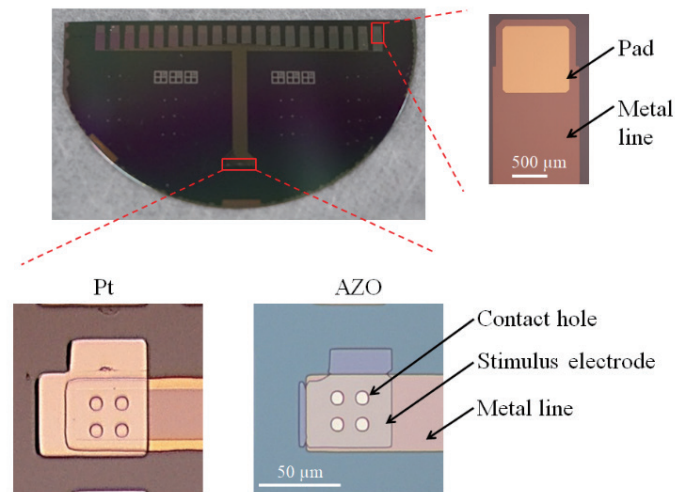


Fig. 4. (Color online) Microphotographs of fabricated test sample with Al-doped ZnO electrodes.

L-shaped materials were the stimulus electrodes whose area was  $4500 \mu\text{m}^2$ . The Al-doped ZnO film was perfectly transparent in the visible wavelength range. A test sample with Pt stimulus electrodes was also fabricated as a reference.

We evaluated the thin film property and stimulus electrode property. The thin film property was evaluated by X-ray diffraction (XRD) and optical measurements. XRD and optical measurements were performed with the test sample with 300-nm-thick Al-doped ZnO deposited on the Si wafer without a Ti/Au/Ti wire and a photolithography process. The diameter of the test sample was 2 inch. The stimulus electrode property was evaluated with the test samples, which have the Al-doped ZnO electrodes. The evaluations were performed using one sample that was fabricated by conventional methods based on the semiconductor process. Therefore, we predict that the deviation of the evaluation results is very small.

### 3. Evaluation Results and Discussion of Al-doped ZnO Transparent Stimulus Electrode

Figure 5 shows the resistivity of the Al-doped ZnO thin film formed with various substrate temperatures. An at least  $200 \text{ }^\circ\text{C}$  substrate temperature was necessary to obtain a lower resistivity of around  $1 \text{ m}\Omega\cdot\text{cm}$ . XRD profiles of the Al-doped ZnO thin films formed at different substrate temperatures were measured and shown in Fig. 6. In the XRD profile, several strong peaks existed for substrate temperatures of 200 and  $300 \text{ }^\circ\text{C}$ . Both Al-doped ZnO thin films had strong ZnO(002) peaks at  $34.34^\circ$ , showing good crystallinity. Meanwhile, there were other peaks in the thin film with a substrate temperature of  $300 \text{ }^\circ\text{C}$ . Figure 7 shows the full width at half maximum of the ZnO(002) peak in the Al-doped ZnO thin film formed with various substrate temperatures. It was clearly indicated that the annealing process was strongly required for the good crystallinity of the Al-doped ZnO thin film. Transparent characteristics

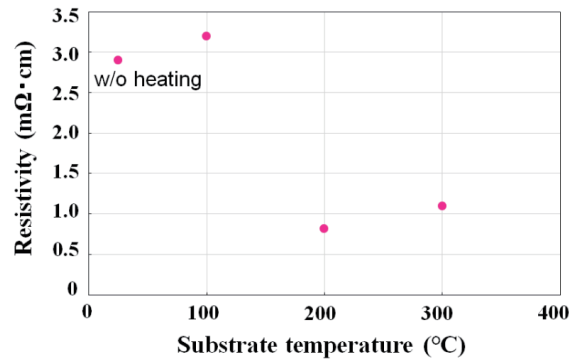


Fig. 5. (Color online) Resistivity of Al-doped ZnO thin film formed with various substrate temperatures.

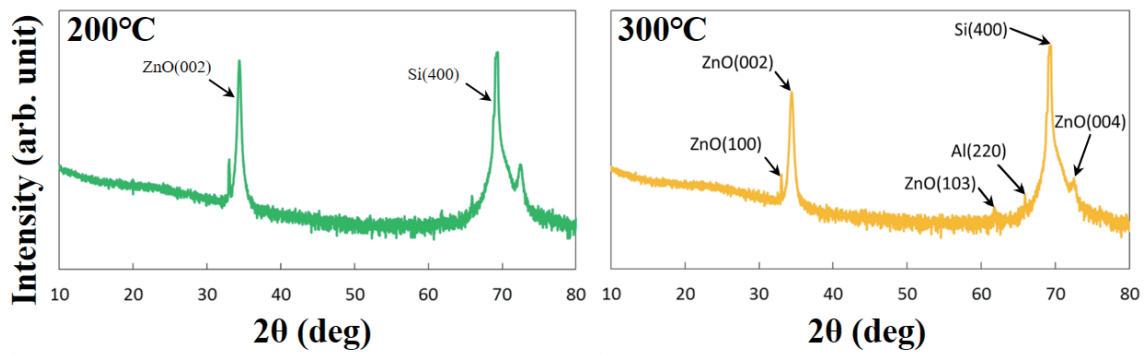


Fig. 6. (Color online) XRD profiles of Al-doped ZnO thin films formed at different substrate temperatures.

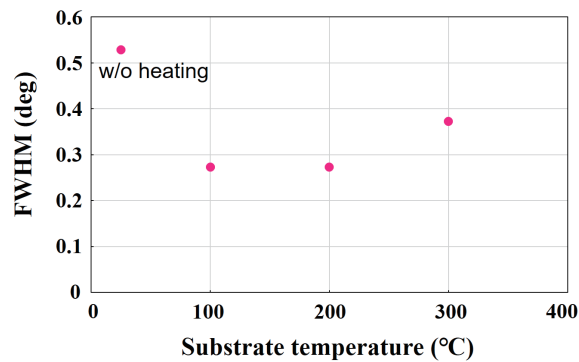


Fig. 7. (Color online) Full width at half maximum of ZnO(002) peak in Al-doped ZnO thin film formed with various substrate temperatures.

were also investigated with an ellipsometer (Horiba, UVISEL-LT-NIR), as shown in Fig. 8. Transmittances of more than 85% in the visible range were observed for the Al-doped ZnO thin film with substrate temperatures less than 200 °C. Meanwhile, the transmittance property degraded with a substrate temperature of 300 °C. Consequently, these results indicated that Al-doped ZnO with a substrate temperature of 200 °C had a better thin film property.

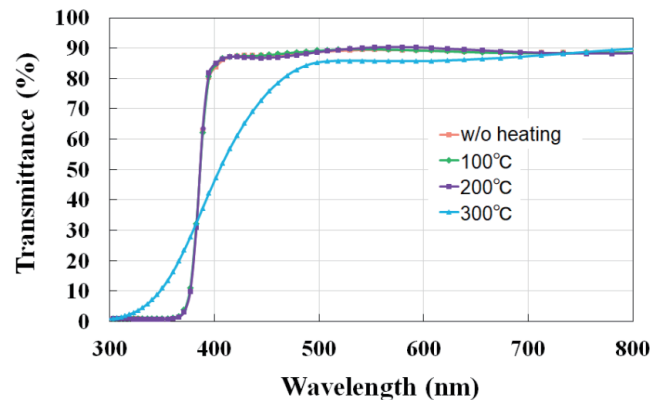


Fig. 8. (Color online) Transmittance of 300-nm-thick Al-doped ZnO thin film formed with various substrate temperatures.

Next, the test samples were characterized to evaluate the stimulus electrode property. Figure 9 shows the electrochemical impedance characteristics of Al-doped ZnO and Pt stimulus electrodes formed with various substrate temperatures. The electrochemical impedances of the stimulus electrodes were measured in a conventional setup with 0.01 M phosphate-buffered saline (PBS) at 23 °C. The working electrode, reference electrode, and counter electrode were the fabricated stimulus electrode, Ag/AgCl electrode, and 2-in. Pt-coated Si wafer, respectively. Measurements were performed with 10 mV AC signals and with frequency ranges from 100 Hz to 100 kHz in PBS used as the electrolyte. For Al-doped ZnO electrodes with different substrate temperatures, the impedance values were approximately 300 k $\Omega$  at a frequency of 1 kHz, which was several times larger than that of the Pt electrode. As a low electrochemical impedance is generally preferable for the stimulus electrode, it was necessary for the Al-doped ZnO stimulus electrodes to lower the impedance values.

CIC was one of the most important properties for the stimulus electrodes. CIC was the maximum injectable charge density that kept the electrode potential within the potential window.<sup>(18)</sup> It was reported that the charge injection of more than 2 nC was necessary in an electrical stimulation to elicit visual sensations for blind patients.<sup>(10,11)</sup> Accordingly, CIC values of more than 0.04 mC/cm<sup>2</sup> are necessary for the fabricated stimulus electrodes. Figure 10 shows the CIC values of Al-doped ZnO and Pt stimulus electrodes formed with various substrate temperatures. CIC values were measured by a conventional method with 0.01 M PBS at 23 °C.<sup>(19)</sup> The used-input biphasic current pulse consisted of a 200  $\mu$ s positive current pulse, a 200  $\mu$ s negative current pulse, and a 20  $\mu$ s interval between the positive and negative current pulses. In general, the input current depends on the maximum cathodic potential ( $E_{mc}$ ) of the electrode material. The  $E_{mc}$  of the Al-doped ZnO was approximately -1.5 V, which was measured by cyclic voltammetry. Then, the recorded electrode potential (vs Ag/AgCl) range was from approximately -3 to 2 V. It was indicated that the Al-doped ZnO stimulus electrodes had adequate CIC values of more than 0.07 mC/cm<sup>2</sup> for the evocation of visual sensations. In these experiments, there was no clear relationship between the thin film properties and the electrical characteristics in Al-doped ZnO. Detailed studies are needed to achieve lower electrochemical

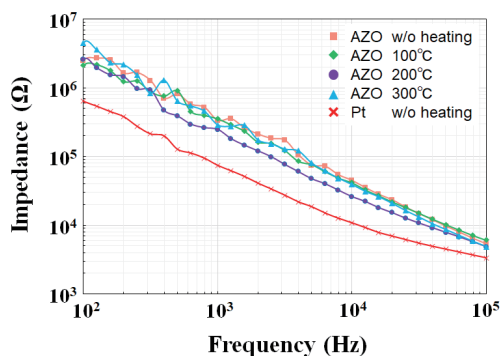


Fig. 9. (Color online) Impedance characteristics of Al-doped ZnO and Pt stimulus electrodes formed with various substrate temperatures.

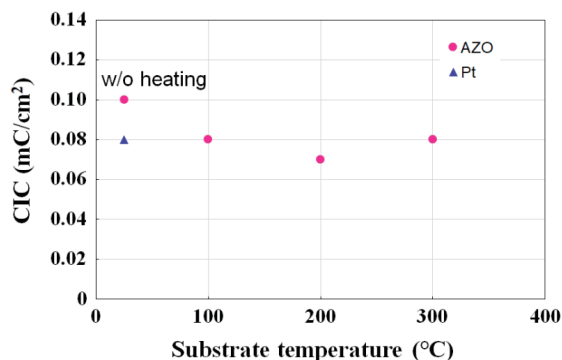


Fig. 10. (Color online) CIC values of Al-doped ZnO and Pt stimulus electrodes formed with various substrate temperatures.

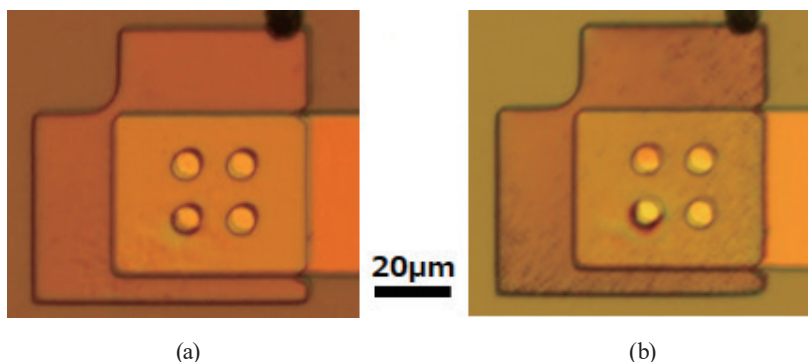


Fig. 11. (Color online) Microscopy images of the surface of the Al-doped ZnO electrode (a) before and (b) after the electrochemical measurements.

impedances and higher CIC values. Figure 11 shows a microscopy image of the electrode surface of the Al-doped ZnO before and after the electrochemical measurements. We observed that the material surfaces barely changed before and after the electrochemical measurements.

#### 4. Conclusions

The fundamental characteristics of the Al-doped ZnO transparent stimulus electrode were studied to realize a 3D stacked retinal prosthesis chip with the large stimulus electrode area and large photodiode area simultaneously. The test samples were fabricated to evaluate the thin film property and stimulus electrode property. The Al-doped ZnO thin film had both crystallinity and transmittances depending on the substrate temperature during thin-film formation. Experimental results indicated that the Al-doped ZnO with a substrate temperature of 200 °C had a good crystallinity and a transmittance of more than 85% in the visible range. The Al-doped ZnO stimulus electrode also had both good electrochemical impedance characteristics and adequate CIC values of 0.07 mC/cm<sup>2</sup> to evoke visual sensations. As a result, Al-doped ZnO has the possibility of becoming the transparent stimulus electrode of the 3D stacked retinal prosthesis chip although detailed studies including biocompatibility are also necessary.



## Acknowledgments

This work was supported by the Japan Society for the Promotion of Science (JSPS), Grant-in-Aid for Scientific Research (A), No. 15H01812. This work was performed in the Micro/Nano-Machining Research and Education Center, Tohoku University.

## References

- 1 G. A. Stevens, R. A. White, S. R. Flisman, H. Price, J. B. Jonas, J. Keeffe, J. Leasher, K. Naidoo, K. Pesudovs, S. Resnikoff, H. Taylor, and R. A. Boume: *Ophthalmology* **120** (2013) 2377.
- 2 N. E. Medeiros and C. A. Curcio: *Invest. Ophthalmol. Vis. Sci.* **42** (2001) 795.
- 3 M. S. Humayun, E. Juan, J. E. Weiland, G. Dagnelie, S. Katona, R. Greenberg, and S. Suzuki: *Vision Res.* **39** (1999) 2569.
- 4 W. Liu, K. Vichienchom, M. Clements, S. C. DeMarco, C. Hughes, E. McGucken, M. S. Humayun, E. DeJuan, J. D. Weiland, and R. Greenberg: *IEEE J. Solid-State Circuits* **35** (2000) 1487.
- 5 J. Ohta, N. Yoshida, K. Kagawa, and M. Nunoshita: *Jpn. J. Appl. Phys.* **41** (2002) 2322.
- 6 M. Koyanagi, Y. Nakagawa, K.-W. Lee, T. Nakamura, Y. Yamada, K. Inamura, K.-T. Park, and H. Kurino: *Int. Solid-St. Circ. Conf. Tech. Dig.* (2001) 270.
- 7 T. Tanaka, T. Kobayashi, K. Komiya, K. Sato, T. Watanabe, T. Fukushima, H. Tomita, H. Kurino, M. Tamai, and M. Koyanagi: *Tech. Dig. IEEE Int. Electron Dev. Meet.* (2007) 1015.
- 8 M. S. Humayun, J. D. Dorn, A. K. Ahuja, A. Caspi, E. Filley, G. Dagnelie, J. Salzmman, A. Santos, J. Duncan, L. daCruz, S. Mohand-said, D. Elliott, M. J. McMahon, and R. J. Greenberg: *Proc. Eng. Med. Biol. Soc.* (2009) 4566.
- 9 M. S. Humayun, J. D. Dorn, L. da Cruz, G. Dagnelie, J. Sahel, P. E. Stanga, A. V. Cideciyan, J. L. Duncan, D. Elliott, E. Filley, A. C. Ho, A. Santos, A. B. Safran, A. Arditi, L. V. Del Priore, and R. J. Greenberg: *Ophthalmology* **119** (2012) 779.
- 10 E. Zrenner, K. U. Bartz-Schmidt, H. Benav, D. Besch, A. Bruckmann, V. Gabel, F. Gekeler, U. Greppmaier, A. Harscher, S. Kibbel, J. Koch, A. Kusnyerik, T. Peters, K. Stingl, H. Sachs, A. Stett, P. Szurman, B. Wilhelm, and R. Wilke: *Proc. R. Soc. London, Ser. B.* **278** (2011) 1489.
- 11 E. Zrenner, K. U. Bartz-Schmidt, H. Benav, D. Besch, A. Bruckmann, S. Danz, V.-P. Gabel, F. Gekeler, H.-G. Graf, U. Greppmaier, A. Harscher, G. Hoertdoefer, S. Kebbel, U. Klose, A. Kopp, A. Kusnyerik, W. Nisch, T. Peters, D. Rathbun, S. Reinert, K. Stingl, H. Sachs, I. Sliesoraityte, A. Stett, P. Szurman, B. Wilhelm, R. Wilke, and W. Wrobel: *Electronic Supplementary Material to the publication of E. Zrenner et al.: Subretinal electronic chips allow blind patients to read letters and combine them to words. Electron Suppl. Mater. Proc. R. Soc. London, Ser. B.* **278** (2011) 1489.
- 12 K. Stingl, K. U. Bartz-Schmidt, D. Besch, A. Braun, A. Bruckmann, F. Gekeler, U. Greppmaier, S. Hipp, G. Hörtdörfer, C. Kernstock, A. Koitschev, A. Kusnyerik, H. Sachs, A. Schatz, K. T. Stingl, T. Perters, B. Wilhelm, and E. Zrenner: *Proc. R. Soc. London, Ser. B* **280** (2013) 20130077.
- 13 T. Fujikado, M. Kamei, H. Sakaguchi, H. Kanda, T. Morimoto, Y. Ikuno, K. Nishida, H. Kishima, T. Maruo, K. Konoma, M. Ozawa, and K. Nishida: *Invest. Ophthalmol. Vis. Sci.* **52** (2011) 4726.
- 14 G. A. Mohammad and M. Behrooz: *Iran. Biomed. J.* **15** (2011) 38.
- 15 D. Yingrui, P. A. Denls, Z. K. Jerzy, and S. M. Greg: *Anal. Chem.* **79** (2007) 7526.
- 16 B. J. Zhou, N. Xu, and Z. L. Wang: *Adv. Mater.* **18** (2006) 2432.
- 17 H.-W. Wu, C.-H. Chu, Y.-F. Chen, Y.-W. Chen, W.-H. Tsai, S.-H. Huang, and G.-S. Chen: *Proc. Int. Mult. Conf. Eng. Comp. Sci. II* (2013) 13.
- 18 S. F. Cogan: *Annu. Rev. Biomed. Eng.* **10** (2008) 275.
- 19 K. Ito, S. Uno, T. Goto, Y. Takezawa, T. Harashima, T. Morikawa, S. Nishino, H. Kino, K. Kiyoyama, and T. Tanaka: *Jpn. J. Appl. Phys.* **56** (2017) 04CM05.

## About the Authors



**Hisashi Kino** received his B.S., M.S., and Ph.D. degrees from Tohoku University, Japan, in 2007, 2009, and 2012, respectively. Since 2012, he has been an assistant professor at Tohoku University, Japan. He is currently an assistant professor at the Frontier Research Institute for Interdisciplinary Sciences, Tohoku University, Japan, and a visiting assistant professor at the Department of Electrical Engineering, Stanford University, CA, USA. His research interests are in semiconductor memory, 3D integration technology, and sensors.



**Takafumi Fukushima** received his Ph.D. degree from the Department of Materials Science and Chemical Engineering of Yokohama National University, Japan, in 2003. From 2004 to 2009, he was an assistant professor at the Department of Bioengineering and Robotics, Tohoku University. Since 2010, he has been an associate professor at NICHe, Tohoku University. From 2016 to 2017, he was a visiting faculty with the University of California, Los Angeles. He is currently an associate professor at the Department of Mechanical Systems Engineering, Tohoku University, and a visiting faculty at the Center for Heterogeneous Integration and Performance Scaling, University of California, Los Angeles. His research interests include 3D and heterogeneous system integration including through-silicon via, capillary self-assembly, multichip-to-wafer bonding, and flexible fan-out wafer-level packaging technologies.



**Tetsu Tanaka** received his B.S. and M.S. degrees in electronics engineering and Ph.D. degree in machine intelligence and systems engineering from Tohoku University, Sendai, Japan, in 1987, 1990, and 2003, respectively. In 1990, he joined Fujitsu Laboratories, Ltd. From 1994 to 1995, he was a visiting fellow at the University of California, Berkeley. In 2005, he moved to Tohoku University as an associate professor, and became a professor at the Graduate School of Biomedical Engineering, Tohoku University, in 2008. At Tohoku University, he is working on the research and development of integrated biomedical micro/nano devices and systems using semiconductor technologies and neural engineering. His research topics include intelligent Si neural probes, fully implantable retinal prosthesis system, 3D-IC technology, and analog/digital LSI designs.